

P *LVV* and *LMM* Auger emission induced by Ar⁺ impact on the InP(110) surface

S. Valeri, M. Liberi, and R. Verucchi

Istituto Nazionale per la Fisica della Materia and Dipartimento di Fisica, Università di Modena, via Campi 213/a, 41100-Modena, Italy

(Received 9 May 1997)

The ion-stimulated Auger electron emission from P atoms was used to study collisional processes and core excitation in InP following bombardment with 1–10 keV Ar⁺ in oblique incidence. Both the line shape and the yield of the P *LVV*, bulklike emission and of the P *LMM*, atomiclike emission were investigated. It has been found that core excitations mainly originate in asymmetric collisions at all bombarding energies above threshold. The dependence of the sputtering yield on the ion incidence angle has been found to contribute significantly to the angular distribution of the P *LMM* partial yield. [S0163-1829(97)02747-1]

I. INTRODUCTION

Inelastic interactions of nonreactive, low-energy (keV) ions with surfaces have been extensively reviewed in the last decade.^{1–5} They include both electronic and kinematic processes. When the kinetic energy of the colliding particles is high enough to allow the formation of an instantaneous quasimolecule, very large excitation cross sections can occur by promotion of inner-shell electrons through crossing of molecular orbitals.^{6,7} The subsequent decay would result in Auger spectra very similar to the electron- and photon-excited cases, owing to the substantial insensitivity of the Auger decay to the ionization process. However, kinematic processes also occur, namely, ejection of target particles by momentum transfer in direct (projectile-target) or secondary (target-target) collisions (sputtering).⁵ Sputter-ejected, excited particles decay outside the solid, resulting in an “atomiclike” spectral distribution superimposed to the “bulklike” distribution originated from decay into the solid.

Such a kinetic electron emission has been investigated in a number of elements, alloys, and compounds, but most of the work has been focused on Mg, Al, and Si, because of the very high excitation cross section in these light elements.^{1–3} Phosphorous has been less fully investigated, although it exhibits a large cross section for the ion-induced, core-level ionization process.^{8,9}

We report in this paper on a detailed study of the phosphorous Auger emission induced by impact of Ar ions of 1–10 keV energy on the (110) surface of InP, in order to get insight on the sputter-related collisional and emission processes. The interaction of ions with the surface of InP (and other III-V compound semiconductors) is in fact a widely investigated but not fully understood process.^{10–12} Surface sensitivity of the ion-induced electron emission has been recently outlined;^{13,14} therefore, this approach is suitable for study of collisions in the outermost layers.

II. EXPERIMENT

The (110) surface of InP was prepared by cleavage in UHV (base pressure lower than 2×10^{-10} Torr). Electron emission was detected by a cylindrical mirror analyzer (CMA), 0.3% resolution, operating in the first derivative mode. For line-shape measurements, a 1 V modulation was

used, while for yield measurements a modulation of 8 V was used. The conventional Auger electron emission (electron-induced Auger emission, EAE) was excited by the electron gun coaxial to the CMA analyzer. The current was 0.5 μA in a spot 10 μm in diameter. The ion-induced Auger emission (IAE) was excited by a differentially pumped ion gun operating at energy E_p of 1–10 keV. The ion current density was of the order of $10^2 \mu\text{A cm}^{-2}$. Ion guns generally produce a significant amount of doubly charged particles, which can affect the measurement of the yield versus energy, in particular where the threshold estimation is concerned.^{3,15} However, the multicharged ions fraction can be drastically reduced using an appropriate ionizing discharge voltage (30–50 V in the present case).^{15,16}

Due to the marked dependence of IAE emission on the experimental geometry (the ions' incidence angle and the electrons take-off angle),^{1–3,17–20} measurements were performed in well-defined geometries. Basically, an ion incidence angle of 65° with respect to the surface normal was used for yield measurements, and the electrons were collected using the full angular acceptance of the CMA, but experiments were also performed at different incidence angles. The line-shape measurements were performed at an ion incidence angle of 65° using two different take-off geometries to emphasize Doppler-related contributions.^{18,20} To this end, two distinct, narrow acceptance cones, centered at -45° and $+45^\circ$ from the surface normal in the plane defined by the ion-beam direction and the surface normal, were selected by mechanical shields. We will refer in the following to these geometries as to “backward” and “forward” geometry, respectively.

III. RESULTS AND DISCUSSION

A. Line-shape study

The ion-excited phosphorous Auger emission is shown in Fig. 1, for the InP surface bombarded with 3 keV Ar ions in grazing incidence and backward take-off angle, in both the first derivative form [panel (a)] and the integral, background subtracted form [panel (b)]. For comparison, the electron-excited *LVV* emission is also shown. The EAE spectrum primarily reflects the self-folded valence density of states at the core-hole excited site.^{21,22} The dominant feature at 119 eV is related to transitions leaving two holes of *p* symmetry

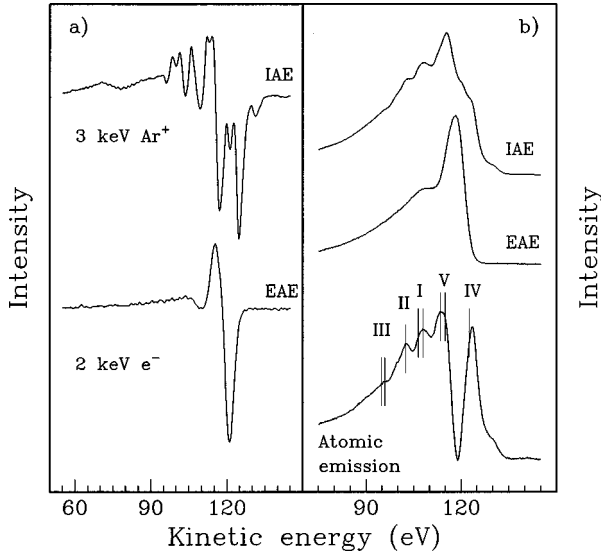


FIG. 1. Energy distribution of P electrons emitted by 5 keV Ar⁺ (IAE) and 1 keV electron bombardment (EAE) of the InP(110) surface at oblique incidence. (a) The first derivative spectrum and (b) the background-subtracted integral spectrum are shown. In the (b) panel the atomic, *LMM* contribution to the full IAE spectrum is also shown (bottom curve). Calculated energies of the P *LMM* Auger transitions (see Table I) are indicated by markers.

in the valence band, while the shoulder on the low kinetic-energy side (between 100 and 115 eV) is mainly *sp* and *pp* derived. Inelastic losses also contribute to the spectral intensity in this energy range.

The IAE spectrum also originates in the decay of the $2p$ core holes. Main peaks are located at about 115, 107, and 102 eV, respectively. A relevant shoulder is present on the high kinetic-energy (KE) side. A minor feature is detectable at about 95 eV. As in the Mg, Al, and Si case, however, the dominant features do not originate in the *LVV*, bulklike emission, but in the *LMM*, atomic emission.

Separation of *LVV* and *LMM* contribution can be done by subtracting the EAE spectrum from the IAE one, in the assumption that the *LVV* component is satisfactorily described by the Auger spectrum obtained under electron bombardment.^{1,2} The magnitude of the electron-induced spectrum is conveniently adjusted to fit the IAE spectrum. The result of such a procedure is shown in Fig. 1(b), lower curve. The percentage weight of atomic and bulk intensity with respect to the total yield is 25% and 75%, respectively, as measured from the area of the *LMM* and *LVV* spectra. Peaks in the *LMM* spectrum are labeled according to the Al and Si *LMM* spectrum.²³ We assigned the atomiclike peaks to specific Auger transitions in either ionized (initial state $2p^5 3s^2 3p^3$) or neutral excited (initial state $2p^5 3s^2 3p^4$) sputtered particles, as already done in the literature for Mg, Al, and Si.^{23,24} The decay of atoms with a double $2p$ vacancy and an additional electron in the outer shell (initial state $2p^4 3s^2 3p^4$) is also considered, which roughly correspond to peak IV in the experimental spectrum. Some calculated Auger transition energies are given in Table I and are indicated by vertical markers in Fig. 1(b), lower curve. In singly ionized P atoms (P⁺), energies have been evaluated from tabulated data of ionization potentials.²⁵ For P neutral atoms (P⁰) the energy difference between $2p^5 3s^2 3p^4$ and

TABLE I. Calculated Auger transition energies.

Transitions from		to	Calculated values (eV)		
P ⁺	$2p^5 3s^2 3p^3$	\Rightarrow	$2p^6 3s 3p^3$	² P	95.8
				² S	96.9
				⁴ P	102.3
P ⁰	$2p^5 3s^2 3p^4$	\Rightarrow	$2p^6 3s 3p^3$	¹ D	107.5
				³ P	107.6
				³ D	109
				¹ S	114.5
				¹ D	116
P ²⁺	$2p^4 3s^2 3p^4$	\Rightarrow	$2p^5 3s^2 3p^3$		123.5

$2p^6 3s 3p^3$ or $2p^6 3s^2 3p^2$ states can be well approximated to the energy difference between $2p^6 3s^2 3p^4$ and $2p^6 3s 3p^3$ or $2p^6 3s^2 3p^2$ states of the next-highest element in atomic number (sulfur, in the present case).²⁶ For doubly ionized P atoms (P²⁺) with initial state $2p^4 3s^2 3p^4$, energies have been evaluated using the same rule, although a larger uncertainty might be expected.

The most relevant feature in the P atomiclike emission is peak I, however, the relative weight of peak V is larger in the *LMM* spectrum of P with respect to the Al and Si case. Peak V has its origin in a *p-p* transition (see Table I) from a neutral-excited initial state; therefore its intensity reflects the increasing occupancy of the $3p$ level. It is, in fact, absent in Mg, where the excited atom has only one $3p$ electron, and it is maximum in P. The relative intensity of the ion-related *LMM* emission (peaks II and III) with respect to the neutral-related emission (peaks I and V) is larger in the InP spectrum in comparison to, e.g., the Si one.^{23,24,27} Also, the relative intensity of peak IV with respect to the total *LMM* emission is larger in comparison to the Al and Si case.^{23,24,27} Similar trends have been observed for Si *LMM* emission on passing from pure Si to silicon-metal compounds;²⁷ therefore both these results are possibly related to the occurrence of P emission in the InP compound. The large intensity of peak IV indicates that asymmetric collision are important in the P $2p$ core ionization at all the bombarding energies above threshold. In fact this peak is associated to the decay of P atoms having two $2p$ holes and therefore originates in asymmetric (Ar-P or In-P) collisions only.¹⁷

The 3 keV, atomic IAE spectra in backward and forward geometries are compared in Fig. 2 (curves *a*, and *b*, respectively). The difference curve is also shown, indicating that the “forward” spectrum is a superposition of the “backward” one and a spectrum similar in shape but rigidly shifted to the high KE side. The dependence of the IAE line shape on the take-off angle has already been reported and discussed in detail.^{18–20} It is ascribed to a Doppler effect that apparently changes the KE of the emitted electrons from sputter-ejected atoms moving with a large component of its velocity toward the analyzer. Shifted features indicate also in InP the occurrence of a strong asymmetry in the kinetic and spatial distribution of sputter-ejected particles, in particular the presence of a highly directional flux of high-energy particles nearly specular to the incident ion beam, in strict similarity with the Al and Si case.^{1–3,18–20}

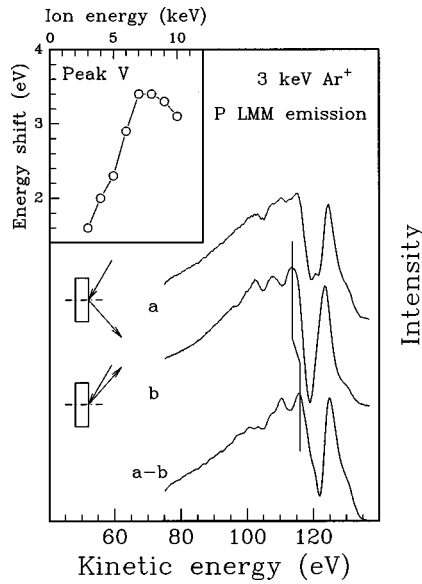


FIG. 2. Energy distribution of P *LMM* Auger electrons in forward and backward take-off geometry (curve *a* and *b*, respectively), for 3 keV Ar^+ in oblique incidence. The *a-b* difference curve represents the Doppler-related contribution to the atomic emission in forward geometry. Curves are normalized in intensity. The energy shift of the peak *V* in forward geometry with respect to the backward geometry is shown in the inset as a function of the ion energy.

The energy shift of the Doppler contributions markedly depends on the KE of ions;^{2,18,19} therefore the IAE line shape in forward geometry also depends on the KE of projectiles. The energy shift of the peak *V* of P *LMM* spectrum in forward geometry with respect to the same peak in backward geometry is shown in Fig. 2(b) as a function of the KE of Ar^+ projectiles. The shift increases with the ion energy in the 2–7 keV range moving from 1.5 to 3.4 eV, then reduces to 2.7 eV at 10 keV. Maximum shift corresponds to a KE of the emitters of about 1.5 keV. The shift reduction between 7 and 10 keV is possibly related to an increasing presence of clusters in the energetic, ejected flux. The velocity of P clusters with *n* P atoms should be $\approx n^{-1/2}$ of that of single P atoms. Then, the emission of an increasing number of clusters with *n*=2 and 3 will result in a progressively reduced Doppler shift, just the effect we observed at large KE of projectiles. A significant presence of clusters in the sputter emission has been reported for Ar^+ bombardment of Si (Refs. 28–30) and metallic targets.³¹

B. Auger yields

The total yield of the P IAE emission is shown in Fig. 3 as a function of E_p . Values are normalized to the 10 keV one. The near-threshold energy region is shown in detail in the inset of Fig. 3. The P IAE emission energy threshold E_{th} can be located between 1 and 1.4 keV, when the IAE signal intensity is comparable to the noise. Value of threshold has been reported to increase with the atomic number of the emitter.³² In compounds, it has been shown to be similar^{33,34} or slightly exceeds³⁵ that for the pure element. For Si IAE emission, values between 0.6 and 1 keV have been reported, in Si and in transition-metal silicides. Our results show that

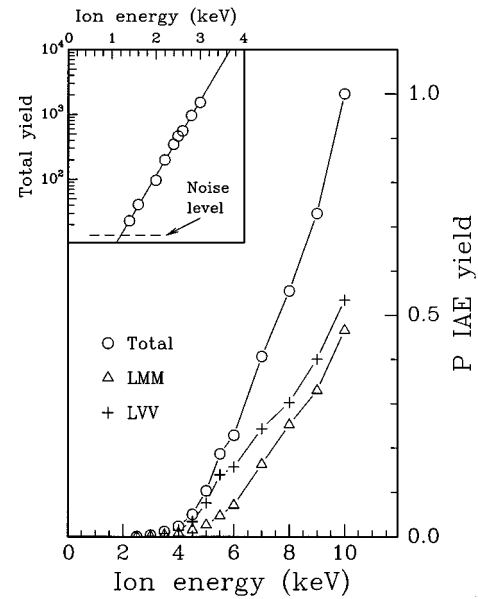


FIG. 3. IAE P yield as a function of the ion energy. Total yield is shown, in comparison with both the *LVV* and the *LMM* contributions. Values are normalized to the total yield value at 10 keV. The inset shows in more detail the energy-threshold region. Arrows indicate the noise level that has been assumed to be the zero value for the IAE yield measurement.

the threshold of P IAE emission is similar to that of Si. The P total yield increases with E_p , as already observed on other targets.^{33,36–39} In Si and Al two distinct regions were found, characterized by a different dependence of the yield on $E_p - E_{th}$. The quadratic dependence observed up to about 3 keV was ascribed to the dominance of target-target symmetric collisions, while the onset and the increasing importance of the asymmetric projectile-target collisions at larger energy results in an overquadratic dependence of the yield on $E_p - E_{th}$. The IAE total yield curve of Fig. 3 shows a nearly cubic dependence on $E_p - E_{th}$ over the full energy range we explored. The energy dependence of the *LVV* and *LMM* components is also shown. The behavior is qualitatively similar. Therefore we conclude that the P IAE emission in InP mainly originates in asymmetric P-*T* collisions even in the near-threshold energy range, as already deduced in the previous section on the basis of the IAE line-shape analysis. This conclusion is in contrast with a number of experimental and computational findings on other targets.^{2,19,33,35,37–39} It is however, in agreement with recent molecular-dynamics simulation of collisional excitation mechanisms in Al.⁴⁰ It has been reported that core excitation proceeds predominantly by asymmetric collisions at all bombarding energies above threshold.

In spite of the qualitatively similar trend versus E_p of the *LVV* and *LMM* yields, the *LVV/LMM* yield ratio shows a nonmonotonic behavior versus E_p . The intensity of the bulk contribution increases more rapidly than the intensity of the atomic one up to 5 keV, then the trend is reversed, resulting in a maximum in the *LVV/LMM* ratio as a function of E_p [Fig. 4(a)]. Qualitatively similar results have been reported for Si,^{29,36} and are shown in Fig. 4 in comparison with the present ones for P. The Si sputtering yield is almost constant in this energy range; therefore the maximum in the Si curve

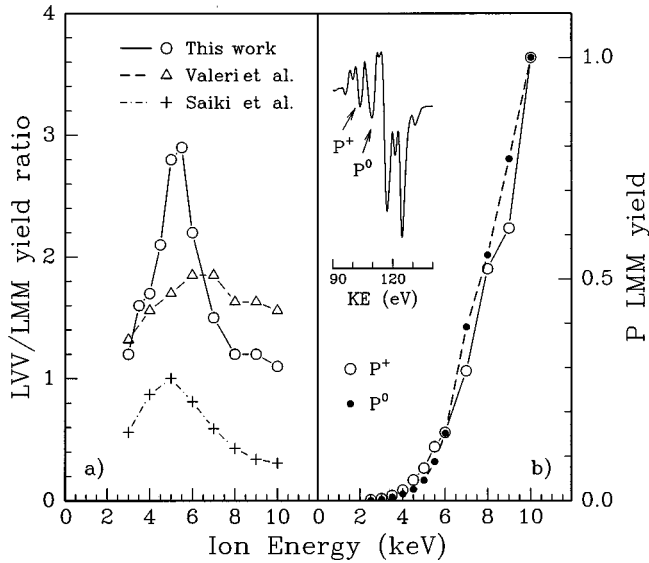


FIG. 4. (a) *LVV/LMM* P yield ratio as a function of the ion energy. Results for Ar⁺ bombardment of Si surface are also shown from the literature (Refs. 28 and 36). (b) *LMM* P yield as a function of the ion energy. The contributions from ionized and neutral-excited sputtered atoms are shown, normalized at 10 keV. The P⁺ and P⁰ yields were measured as the HPP of the 102 and 109 eV features in the first derivative form of the IAE spectrum, as shown in the inset.

has been attributed to the firstly increased, then reduced efficiency of the bulk related emission when the cascade first progressively develops within the depth that corresponds to the electron inelastic mean-free path, then expands deeper. A similar explanation also holds for the P results. The larger value of the maximum in the *LVV/LMM* curve for P emission in InP with respect to the Si case is ascribable to the differences in the cascade development in the two materials, and to the different value of the inelastic mean free path of P and Si Auger electrons. It has been shown in fact that, although the IAE emission yield in the low-energy region is controlled by the generation volume, at energies larger than 2 keV the interplay between the generation and the emission volume becomes important.^{13,14} Monte Carlo simulations⁴¹ that we performed in the 2–7 keV range suggested that the collisional cascade development is weaker and deeper in Si with respect to InP. Due also to the shorter inelastic mean free path of Si Auger electrons with respect to the P ones, the collisional cascade has therefore a reduced efficiency, resulting in a reduced efficiency of the bulk-related emission.

In Fig. 4(b), two components of the yield are shown as a function of E_p , namely, peaks I and II, originating in neutral excited atoms decay or ionized atoms decay, respectively. Values are normalized at 10 keV. The strictly similar behavior suggests that the charge state of particles in the sputtered flux is almost independent on E_p .

The IAE yield has also been studied as a function of the ion-beam polar incidence angle θ , in the 25°–65° range, by rotating the sample in front of the ion gun. The IAE yield versus θ is shown in Fig. 5, where the total value and the *LMM* and *LVV* values are comparatively reported. Data were corrected by the angular response of the analyzer. The *LVV* yield largely exceeds the *LMM* one over the full angular range we explored; therefore the total yield substan-

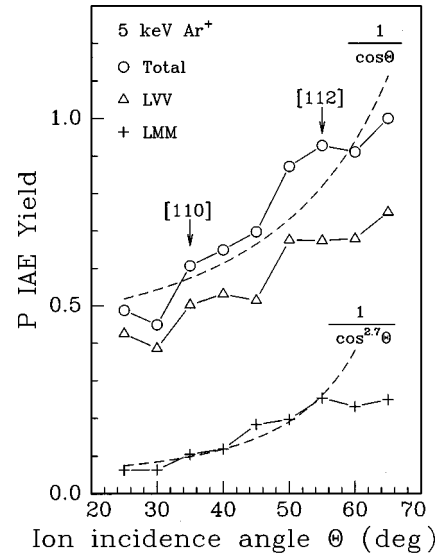


FIG. 5. IAE P yield as a function of the angle of incidence of the 5 keV Ar⁺ beam. The total yield and the *LMM* and *LVV* yield are reported.

tially reflects the partial *LVV* yield angular behavior. The total yield rises as $1/\cos\theta$, as expected because of the increasing path of the ions near the surface with increasing incidence angle. A similar dependence of the IAE yield on the incidence angle has been already reported for the Au(111) surface.⁴² It is well known that ion bombardment of crystalline semiconductors converts the surface layer to the amorphous state; therefore modulation by the lattice, often observed in other systems,^{42–44} is in the present case avoided because the very fast and easy amorphization of InP in the bombardment conditions (large fluence and high energy) we used.^{10,11} However, in the total and even clearly in the *LVV* curve, large bumps are present, in correspondence to the main crystalline directions encompassed by the ion beam, namely, [110] and [112] at 35° and 55°, respectively.

The *LMM* yield deviates from the $1/\cos\theta$ dependence because it also reflects the angular behavior of the sputtering yield. It increases from normal to grazing incidence, up to a maximum, then sharply reduces at very grazing incidence. The maximum has been found in the 55°–70° region for GaAs, GaSb, and GaP,⁴⁵ in reasonable agreement with our finding on InP. For $\theta \leq 50^\circ$, the sputtering coefficient can be approximated by curves of the type $y = 1/(\cos^h\theta)$, where h was found to range from 2 in GaP to 2.8 in GaSb.⁴⁵ In all cases the value is larger than $h = 1.67$ predicted by the Sigmund theory.⁵ The *LMM* curve in Fig. 5 is satisfactorily fitted up to 55° by using $h = 2.7$. At larger angles the *LMM* yield deviates from this dependence and saturates in agreement with the occurrence of a broad maximum nearly located at 70°.

IV. CONCLUSIONS

In conclusion, we have shown the following. (1) P Auger emission stimulated by Ar ions in InP proceeds predomi-

nantly by asymmetric collisions in the whole 1–10 keV energy range. (2) In spite of the overall similarities, spectral differences have been detected in the P IAE emission with respect to the close elements in the Periodic Table (Si, Al, Mg), namely, (i) the relevance of the p - p related emission, and (ii) the dominant contribution from charged, sputtered particles in the P LMM , atomic spectrum. (3) The LVV/LMM yield ratio shows a maximum at 5 keV ion energy, related to the collisional cascade development within the inelastic mean free path of P Auger electrons. (4) The

total yield exhibits a $1/\cos\theta$ dependence on the ion incidence angle θ ; however, the LMM partial yield also reflects the angular behavior of the sputtering yield.

ACKNOWLEDGMENTS

Financial support by Istituto Nazionale per la Fisica della materia (INFN) and by Ministero dell'Università e della Ricerca Scientifica e Tecnologica (MURST) is gratefully acknowledged.

-
- ¹J. Mischler and N. Benazeth, *Scanning Electron Microsc.* **2**, 351 (1986).
- ²S. Valeri, *Surf. Sci. Rep.* **17**, 85 (1993).
- ³R. A. Baragiola, *Nucl. Instrum. Methods Phys. Res. B* **78**, 223 (1993).
- ⁴S. R. Kasi, H. Kang, C. S. Sass, and J. W. Rabalais, *Surf. Sci. Rep.* **10**, 1 (1989).
- ⁵P. Sigmund, in *Sputtering by Particle Bombardment II*, edited by R. Behrish, *Topics in Applied Physics Vol. 47* (Springer, Berlin, 1981).
- ⁶M. Barat and W. Lichten, *Phys. Rev. A* **6**, 211 (1972).
- ⁷D. Schneider, G. Nolte, U. Wille, and N. Stolterfoht, *Phys. Rev. A* **28**, 161 (1983).
- ⁸P. Viaris de Lesegno and J.-F. Hennequin, *Surf. Sci.* **80**, 656 (1979).
- ⁹L. Viel, C. Benazeth, and N. Benazeth, *Surf. Sci.* **54**, 63 (1976).
- ¹⁰J. B. Malherbe, *CRC Crit. Rev. Solid State Mater. Sci.* **19**, 55 (1994).
- ¹¹S. Valeri and M. Lolli, *Surf. Interface Anal.* **16**, 59 (1990).
- ¹²A. M. Mazzone, *Philos. Mag. A* **57**, 741 (1988).
- ¹³R. Verucchi, S. Altieri, and S. Valeri, *Surf. Sci.* **331–333**, 1256 (1995).
- ¹⁴S. Valeri, S. Baraldi, and R. Verucchi, *Surf. Sci.* **365**, 517 (1996).
- ¹⁵R. A. Baragiola, L. Nair, and T. E. Madey, *Nucl. Instrum. Methods Phys. Res. B* **58**, 322 (1991).
- ¹⁶A. Bonanno, N. Mandarino, A. Oliva, and F. Xu, *Nucl. Instrum. Methods Phys. Res. B* **71**, 161 (1992).
- ¹⁷S. Valeri and R. Tonini, *Surf. Sci.* **220**, 407 (1989).
- ¹⁸S. V. Pepper and P. R. Aron, *Surf. Sci.* **169**, 14 (1986).
- ¹⁹R. A. Baragiola, E. V. Alonso, and H. J. L. Raiti, *Phys. Rev. A* **25**, 1969 (1982).
- ²⁰A. Bonanno, F. Xu, M. Camarca, R. Siciliano, and A. Oliva, *Nucl. Instrum. Methods Phys. Res. B* **48**, 371 (1990).
- ²¹R. Weissmann and K. Muller, *Surf. Sci. Rep.* **105**, 251 (1981).
- ²²P. O. Nilsson and S. P. Svensson, *Solid State Commun.* **79**, 191 (1991).
- ²³R. Whaley and E. W. Thomas, *J. Appl. Phys.* **56**, 1505 (1984).
- ²⁴E. W. Thomas, *Vacuum* **34**, 1031 (1984).
- ²⁵C. E. Moore, *Nat. Bur. Stand. (U.S.) Circ. No. 467* (U.S. GPO, Washington, D.C., 1949).
- ²⁶P. Dahl, M. Rodbro, G. Hermann, B. Fastrup, and M. E. Rudd, *J. Phys. B* **9**, 1581 (1976).
- ²⁷S. Valeri and R. Tonini, in *Auger Spectroscopy and Electronic Structure*, edited by K. Wandelt, G. Cubiotti, and G. Mondio (Springer, Berlin, 1988).
- ²⁸S. Valeri and R. Verucchi, *Nucl. Instrum. Methods Phys. Res. B* **59/60**, 37 (1991).
- ²⁹Nandini Ray, P. Rajasekar, and S. D. Dey, *Surf. Sci.* **322**, 90 (1995).
- ³⁰K. Wittmaak, *Nucl. Instrum. Methods Phys. Res. B* **2**, 674 (1984).
- ³¹P. Wurz, W. Husinsky, and G. Betz, *Appl. Phys. A: Solids Surf.* **52**, 213 (1991).
- ³²C. Fan, Z. Yu, and X. Chen, *J. Vac. Sci. Technol. A* **5**, 1206 (1987).
- ³³S. Valeri, R. Tonini, and G. Ottaviani, *Phys. Rev. B* **38**, 13 282 (1988).
- ³⁴S. Valeri and R. Verucchi, *Phys. Scr.* **I41**, 246 (1992).
- ³⁵J. F. Hennequin, R. L. Inglebert, and P. Viaris de Lesegno, *Surf. Sci.* **140**, 197 (1984).
- ³⁶K. Saiki, I. Rittaporn, and S. Tanaka, *Jpn. J. Appl. Phys., Part 1* **26**, 45 (1987).
- ³⁷J. J. Vrakking and A. Kroes, *Surf. Sci.* **84**, 153 (1979).
- ³⁸K. Wittmaak, *Surf. Sci.* **85**, 69 (1979).
- ³⁹M. Iwami, S. C. Kim, Y. Kataoka, T. Imura, A. Hiraki, and F. Fujimoto, *Jpn. J. Appl. Phys.* **19**, 1627 (1980).
- ⁴⁰M. H. Saphiro, T. A. Tombello, and J. Fine, *Nucl. Instrum. Methods Phys. Res. B* **74**, 385 (1993).
- ⁴¹J. F. Ziegler, J. P. Biersack, and U. Littmark, *The Stopping and Range of Ions in Solids* (Pergamon, Oxford, 1985).
- ⁴²D. Rubesame, M. Sternberg, T. Guerlin, and H. Niedrig, *Nucl. Instrum. Methods Phys. Res. B* **59–60**, 80 (1991).
- ⁴³M. Schuster and C. Varelas, *Nucl. Instrum. Methods Phys. Res. B* **9**, 145 (1985).
- ⁴⁴M. Hou, C. Benazeth, N. Benazeth, and C. Mayoral, *Nucl. Instrum. Methods Phys. Res. B* **13**, 645 (1986).
- ⁴⁵N. A. Bert and I. P. Soshnikov, *Phys. Solid State* **35**, 1239 (1993).